

Probing the randomness of ergodic states: extreme-value statistics in the ergodic and many-body-localized phases

Rajarshi Pal

Department of Physics, Sungkyunkwan University, Suwon 16419, Korea.

Arul Lakshminarayan

Department of Physics, Indian Institute of Technology Madras, Chennai, India 600036.

The extreme-value statistics of the entanglement spectrum in disordered spin chains possessing a many-body localization transition is examined. It is expected that eigenstates in the metallic or ergodic phase, behave as random states and hence the eigenvalues of the reduced density matrix, commonly referred to as the entanglement spectrum, are expected to follow the eigenvalue statistics of a trace normalized Wishart ensemble. In particular, the density of eigenvalues is supposed to follow the universal Marchenko-Pastur distribution. We find deviations in the tails both for the disordered XXZ with total S_z conserved in the half-filled sector as well as in a model that breaks this conservation. A sensitive measure of deviations is provided by the largest eigenvalue, which in the case of the Wishart ensemble after appropriate shift and scaling follows the universal Tracy-Widom distribution. We show that for the models considered, in the metallic phase, the largest eigenvalue of the reduced density matrix of eigenvector, instead follows the generalized extreme-value statistics bordering on the Fisher-Tippett-Gumbel distribution indicating that the correlations between eigenvalues are much weaker compared to the Wishart ensemble. We show by means of distributions conditional on the high entropy and normalized participation ratio of eigenstates that the conditional entanglement spectrum still follows generalized extreme value distribution. In the deeply localized phase we find heavy tailed distributions and Lévy stable laws in an appropriately scaled function of the largest and second largest eigenvalues. The scaling is motivated by a recently developed perturbation theory of weakly coupled chaotic systems.

I. INTRODUCTION

The phenomenon of Anderson localisation [1] has been found to survive interactions [2, 3] and a flurry of research activity has been devoted to understanding and characterising this transition to a localized phase from a delocalized or ergodic one. This phenomenon widely referred to as many-body localisation (MBL) is fundamentally interesting as such systems generically break ergodicity and fail to thermalise—thus lying beyond the scope of statistical mechanics. Also, MBL occurs throughout, and especially the middle of the spectrum implying that it is an infinite temperature quantum phase transition, different from usual quantum phase transitions studied at zero temperature [4–7]. These facts combined have significant practical implications for quantum transport [2] and information storage [8, 9]. Experimental advances have allowed the controlled observation of MBL phenomena [10], further driving interest.

Ideas from quantum information have played an important role in the development of the understanding of the ergodic-localized transition. Quantum entanglement, a topic of much importance in quantum information theory, has also gained relevance in quantum many-body physics in the past few years [11, 12]. In particular, the entanglement entropy provides a wealth of information about physical states, including novel ways to classify states of matter that do not have a local order parameter [13, 14]. Many-body eigenstates of thermalizing systems exhibit an entanglement entropy that scales with the volume of the subregion being considered, while many-body eigenstates of many-body localized systems display a boundary law scaling (with possible logarithmic corrections). The study of entanglement entropy and its dynamics has played a crucial role in the elucidation of the properties of the local-

ized and thermal or ergodic phases. Indeed, studies of entanglement entropy [15, 16] provided the first clues as to the emergent integrability of the localized phase. The differences in the nature of multipartite entanglement in the thermal and localized phase is also complementarily reflected in quantities such as a concurrence that measure two qubit entanglements [17]. However, entanglement entropy captures only a small part of the full entanglement structure of a system. Much greater information is contained in the entanglement spectrum [18], from which the entanglement entropy, and much more, maybe extracted.

In the context of MBL, the entanglement spectrum has been studied in some recent papers [19–22] and power laws have been found in disorder averaged Schmidt eigenvalues plotted against the eigenvalue order. In the ergodic phase, different statistical properties of energy levels, such as the ratio of nearest neighbor spacings ([23]) have been shown to correspond to that of one of the canonical random matrix ensembles, the GOE (Gaussian orthogonal ensemble) [7]. In fact going beyond short range correlations the number variance [24, 25] between levels was computed in [26] and was shown to be consistent with the corresponding random matrix theory (RMT) formulae till about 100 mean-level spacings. This together with the claim that the limiting density of eigenvalues of the reduced density matrices of the eigenstates is identical to the Marchenko-Pastur [19] would indicate that deep in the ergodic, delocalized phase, the system is well described by standard random matrix ensembles. A consequence of this is that the eigenstates should be random states and the reduced density matrix (of say k spins out of a total of L) belong to the so-called trace-constrained Wishart ensemble $MM^\dagger/\text{Tr}(MM^\dagger)$, where M is a random matrix of dimension $2^k \times 2^{L-k}$, whose entries are zero-centered independent nor-

mal random numbers. The average entanglement entropy is the von Neumann entropy of such an ensemble and is given by the Page value [27].

It is known that the largest eigenvalues of the Wishart ensemble after a suitable shift and scaling satisfies the universal Tracy-Widom distribution [28], a deviation from the classical extreme value statistics due to the strong correlations of the eigenvalues. On the other hand it is also well known that if a set of random variables are independent and identically distributed then for appropriately rescaled variables there are three possible limiting universal distributions for the extreme maximal events: the Fréchet, Fisher-Tipett-Gumbel, and Weibull distributions [29, 30]. Respectively, they arise depending on whether the tail of the density is a power law, or faster than any power law, and unbounded or bounded. If there are correlations, then it is known that these universal distributions are still valid and reached for sufficiently fast decay of autocorrelations [31]. Thus that the Tracy-Widom law differs from these distributions is the consequence of the peculiar strong correlations present in the eigenvalues of random matrices.

The results of the present paper indicate that the distribution of the maximum of the entanglement spectrum deviates significantly from the Tracy-Widom distribution and instead fits quite well a Fisher-Tipett-Gumbel distribution. This is seen both in a disordered XXZ model with total S_z conserved, which has become a standard model for studying the transition and also in a model with an extra field breaking it which shows the two-component structure [19]. This indicates that correlations in the entanglement spectrum are not Wishart like even deep in the delocalized phase, and perhaps shows signs of pre-localization [32]. Most eigenstates in the metallic state have high entanglement and are delocalized as reflected by the participation ratio. We look at conditional distributions of the maximum eigenvalue of the density matrices filtering only high entropy and participation ratio states and they also follow generalized extreme value distribution (GEV) distributions and not the Tracy-Widom statistic. This is seen to hold even as we start moving towards the transition point but away from it towards the MBL phase, interestingly, the distribution becomes more Fréchet-like. Even when the maximum distribution starts deviating significantly from GEV, we show that the conditional distribution still follows GEV, signaling significant heterogeneity in the spectrum. In the localized phase, we find power laws in the scaled distribution of the largest and second largest eigenvalues. These are quite distinct from the power laws in the disorder averaged entanglement spectra itself plotted against the eigenvalue order [21].

Previous studies on extreme eigenvalues of the reduced density matrices were mostly in the context of strongly chaotic bipartite systems. Remarkable exact results, beyond the asymptotic universal distributions, have been obtained within random matrix theory (RMT) for both the maximum and the minimum eigenvalues and these have been compared with conductance fluctuations in chaotic cavities and entanglement spectra of systems such as coupled kicked tops [33–38]. A study of the transition in the distribution of the largest eigenvalue of the reduced density matrix of eigenstates of chaotic

bipartite systems as a function of interaction, showed that the largest eigenvalue showed deviations from statisticality even when the interactions are strong enough for other statistics to show random matrix behavior [39].

II. PRELIMINARIES: EXTREME-VALUE STATISTICS AND ENTANGLEMENT

This section collects well-known details about extreme-value statistics that are of relevance to this paper, including a discussion of entanglement in random states and the implications for the extreme eigenvalues of the reduced density matrices.

A. Extreme-values of independent or weakly correlated random variables

Let X_1, X_2, \dots, X_N be N observations of an identical independent random variable x with density $p(x)$. Under very general conditions we know from the central limit theorem that the mean $\sum_i X_i/N$ is normally distributed for large N . However, the extremes $(X_{\max})_N = \max\{X_1, X_2, \dots, X_N\}$ and $(X_{\min})_N$ defined similarly are *not* normally distributed, but still show universal behavior. Let,

$$\text{Prob}((X_{\max})_N < x) = F_N(x) =$$

$$\text{Prob}(X_1 < x, X_2 < x, \dots, X_N < x) = \left(\int_0^x p(x) dx \right)^N.$$

For large N , after a shift and change of scale $y = (x - a_N)/b_N$, $F_N(y)$ tends to one of three universal distributions, depending on the tail of the density $p(x)$ [29, 30]. These are

- (i) *Fisher-Tipett-Gumbel*: $\exp(-\exp(-y))$, if the tail of $p(x)$ decays as $\sim e^{-x^\delta}$, $\delta > 0$, faster than a power law,
- (ii) *Weibull*: $\exp(-(-y)^\alpha)$ for $y \leq 0$ and 0 otherwise, if x is bounded above, and the tail of $p(x)$ decays as $\sim |x|^{-1-\alpha}$, $\alpha > 0$,
- (iii) *Fréchet*: $\exp(-y^\alpha)$ for $y \geq 0$ and 0 otherwise, if x is bounded below, and the tail of $p(x)$ decays as $\sim x^{-1-\alpha}$, $\alpha > 0$.

The shift, which is the typical size of the extreme value, and scale parameters a_N and b_N depend on the sample size N and α or δ , in particular for the Fisher-Tipett-Gumbel law, a_N , which follows on requiring that $\int_{a_N}^\infty p(x) dx = 1/N$, is $\sim (\log N)^{1/\delta}$. These distributions can be expressed in a combined way through the generalized extreme value distribution (GEV) with the cumulative distribution function,

$$\begin{aligned} F(y; \xi) &= \exp(-(1 - \xi y)^{1/\xi}) \text{ for } \xi \neq 0 \\ &= \exp(-\exp(-y)) \text{ for } \xi = 0, \end{aligned} \quad (1)$$

with ξ being the shape parameter, $\xi = 0$, $\xi < 0$ and $\xi > 0$ corresponding respectively to the Gumbel, Fréchet and Weibull families.

If the random variables are correlated, then weak correlations in the sense that $\langle x_i x_j \rangle - \langle x_i \rangle \langle x_j \rangle$ is say exponentially small $\sim e^{-|i-j|/\xi}$ with $\xi \ll N$ then the extremes still follow one of the three classical extreme distributions. The maximum intensity in random states, for example, is an exactly solvable case of weakly correlated random variables that limit to the Fisher-Tippett-Gumbel distribution [40]. One well-known case where strong correlations lead to a limiting distribution, the Tracy-Widom distribution, different from the above three classical ones, are the eigenvalues of random matrices [28]. However, for our purposes, we are interested in the singular values of random matrices which are closely connected to entanglement and the largest values also follow the Tracy-Widom distribution [41].

B. Extreme-value statistics, entanglement and the Wishart ensemble

Let us begin by introducing some of the properties of the Wishart ensemble of random matrix theory which is the appropriate ensemble for modelling statistics of the entanglement spectrum. We will discuss the real Wishart ensemble throughout, as the Hamiltonians we consider have time-reversal anti-unitary symmetry [20].

Let, $|\Phi\rangle$ be a state belonging to the tensor product space $\mathcal{H}_1 \otimes \mathcal{H}_2$ with $\dim(\mathcal{H}_1) = n_1$, $\dim(\mathcal{H}_2) = n_2$ and $n_1 \leq n_2$. In our case, since we will be considering entanglement across two $L/2$ partitions of spin-1/2 chains, we will have $n_1 = n_2 = 2^{L/2}$. Let, $\{|i\rangle, |j\rangle\}$ be an orthonormal basis in \mathcal{H}_1 and \mathcal{H}_2 respectively. We have with respect to this basis the state $|\Phi\rangle$ and its Schmidt decomposition,

$$|\Phi\rangle = \sum_{i=1}^{n_1} \sum_{j=1}^{n_2} c_{ij} |i\rangle \otimes |j\rangle = \sum_{i=1}^{n_1} \sqrt{\lambda_i} |i'\rangle_1 |i''\rangle_2. \quad (2)$$

The reduced density matrix of the subsystems are given by $\rho_1 = \text{Tr}_2(|\Phi\rangle\langle\Phi|)$ and $\rho_2 = \text{Tr}_1(|\Phi\rangle\langle\Phi|)$. It follows that Schmidt coefficients λ_i are eigenvalues of $\rho_1 = CC^\dagger$, or equivalently $\rho_2 = (C^\dagger C)^T$ [42], where C is the ‘‘coefficient matrix’’ with elements c_{ij} .

The state is unentangled if and only if $\lambda_1 = 1$ (assuming the Schmidt coefficients are ordered and hence all other eigenvalues are 0), and the Schmidt decomposition gives the states of the individual subsystems. Otherwise $\lambda_2 > 0$ and the Schmidt decomposition consists of at least two terms. For maximally entangled states, $\lambda_j = 1/n_1$ for all j . The entanglement entropy in the state $|\Phi\rangle$ is the von Neumann entropy of the reduced density matrices, $S = -\text{Tr}(\rho_1 \log \rho_1) = -\text{Tr}(\rho_2 \log \rho_2)$. If $S = 0$, then the state is unentangled, while a maximally entangled state has $S = \log n_1$.

Hamiltonians are modeled as random matrices from the GOE in the so called ergodic phase of many-body systems. If the coefficients c_{ij} come from an eigenvector of a typical GOE matrix the induced probability distribution on the Schmidt eigenvalues λ_i and the consequences for entanglement are well-known. [43, 44] The eigenvectors of a matrix

from a GOE of dimension n , are only constrained by normalization and the joint distribution of their components is hence given by,

$$P(x_1, x_2, \dots, x_n) = \frac{\Gamma(n/2)}{\pi^{n/2}} \delta\left(\sum_i x_i^2 - 1\right). \quad (3)$$

Hence, the distribution of c_{ij} is same as that of $[M_{ij}]/\sqrt{\text{Tr}(MM^\dagger)}$ with M being an unstructured matrix with all elements *i.i.d.* zero mean normally distributed numbers, the standard orthogonal ‘‘Ginibre ensemble’’ [45]. Thus the reduced density matrices are given by the ensemble of random matrices,

$$\rho = \frac{MM^\dagger}{\text{Tr}(MM^\dagger)}. \quad (4)$$

These are the so called trace constrained Wishart ensemble of random matrix theory.

The joint probability density function (j.p.d.f.) of λ_i , the eigenvalues of ρ , is

$$P(\lambda_1, \dots, \lambda_{n_1}) = B_{n_1, n_2} \delta\left(\sum_{i=1}^{n_1} \lambda_i - 1\right) \prod_{i=1}^{n_1} \lambda_i^{\frac{\beta}{2}(n_2 - n_1 + 1) - 1} \prod_{j < k} |\lambda_j - \lambda_k|^\beta, \quad (5)$$

where $\beta = 1, 2$ corresponds to real or complex entries of M and B_{n_1, n_2} is a normalization constant known explicitly [24]. The symmetry or Dyson index is $\beta = 1$ for time-reversal symmetric systems such as considered in this paper. There are two sources of correlations in the λ_i , the delta function is a much weaker source of correlation and is identical to that of eigenfunction components as both originate from normalization [40]. The strong and peculiarly RMT correlations arise from the Vandermonde determinant factor involving the product of the differences of every pair of eigenvalues. In the absence of the j.p.d.f. for the eigenvalues of the reduced density matrices of the eigenstates of many-body systems, we want to investigate if the consequences of the strong correlations for the largest eigenvalue are present in the physical systems.

However, before delving into this question, we also investigate the average entanglement and the density of states (of λ_i), which follow from the j.p.d.f.. While an exact result is known for $\beta = 2$: (the Page formula) [27],

$$\langle S \rangle = \sum_{k=n_2+1}^{n_1 n_2} \frac{1}{k} - \frac{n_1 - 1}{2n_2} \approx \ln n_1 - \frac{n_1}{2n_2}, \quad (6)$$

the asymptotic result for large n_1 and n_2 is valid for both $\beta = 1$ and $\beta = 2$.

1. Marchenko-Pastur Law

The average density of the Schmidt eigenvalues is obtained by integrating out all variables except one. For $n_2 \geq n_1 \gg 1$,

with fixed ratio $Q = n_2/n_1 \geq 1$, the limit of the density of scaled eigenvalues $\tilde{\lambda}_i = \lambda_i/n_1$ is given by the Marchenko-Pastur law,

$$\rho_{MP}^Q(x) = \frac{Q}{2\pi} \frac{\sqrt{(x_+ - x)(x - x_-)}}{x}, x_- \leq x \leq x_+,$$

and 0 otherwise. The distribution is in the finite support $[x_-, x_+]$, where $x_{\pm} = 1 + 1/Q \pm 2/\sqrt{Q}$.

For the case $Q = 1$, especially relevant for the numerical results presented, the distribution is given by,

$$\rho_{MP}(x) = \frac{1}{2\pi} \sqrt{\frac{4-x}{x}}, 0 \leq x \leq 4, \quad (7)$$

and zero otherwise. The distribution thus diverges at the origin. The Marchenko-Pastur law is in fact a universal distribution for ensembles of correlation matrices, irrespective of the exact distribution of matrix elements as long as it has a finite moments of sufficiently larger order [46]. The moments of the Marchenko-Pastur distribution, M_n are given by the Catalan numbers,

$$\langle x^n \rangle = C_n = \frac{1}{n+1} \binom{2n}{n},$$

thus $M_n^{1/n} \rightarrow 4$ as $n \rightarrow \infty$ [47].

2. Distribution of maximum eigenvalue

As mentioned earlier, the distribution of the maximum eigenvalue of a Wishart ensemble after suitable centering and scaling follows the Tracy-Widom distribution [28] which has no simple closed-form. For the orthogonal case, it can be defined implicitly by the Hastings-McLeod solution to the second Painlevé equation, [28]. For our purposes, since the reduced density matrix corresponding to a random state has unit trace, we need to adapt the results of the Wishart ensemble to the trace constrained one. This was done in [48], for complex Wishart matrices. Adapting the methods used there with the results of real Wishart matrices in [41] we obtain the same center and scaling in the large n limit as complex matrices, namely a centering or shift of $4/n$ and a scaling equal to $2^{4/3} n^{-5/3}$. This is obtained as follows.

We have our reduced density matrix $\rho = W/S$ (with $W = M^\dagger M$ and $S = \text{Tr}(W)$, Eq. (4)) and thus $\lambda_{\max}(\rho) = \lambda_{\max}(W)/S$. Now, from [41] we know that mean of the distribution of $\lambda_{\max}(W)$, $\langle \lambda_{\max}(W) \rangle$ goes as $(\sqrt{n-1} + \sqrt{n})^2$ while mean of the distribution of trace of W goes as $\langle S \rangle \sim n^2$. Hence, we approximately have the mean of $\lambda_{\max}(\rho)$ equal to, $\langle \lambda_{\max}(\rho) \rangle \sim \frac{(\sqrt{n-1} + \sqrt{n})^2}{n^2} = \frac{4}{n}$, for large n . Again from [41] we know that the standard deviation of the distribution of $\lambda_{\max}(W)$,

$$\sigma_{\lambda_{\max}(W)} \sim (\sqrt{n-1} + \sqrt{n}) \left(\frac{1}{\sqrt{n-1}} + \frac{1}{\sqrt{n}} \right)^{1/3}.$$

As, the fluctuation in the largest eigenvalue is much greater than the fluctuation in the sum of eigenvalues, i.e.,

$$\frac{\sigma_{\lambda_{\max}(W)}}{\langle \lambda_{\max}(W) \rangle} \gg \frac{\sigma_S}{\langle S \rangle}$$

we approximately have, $\sigma_{\lambda_{\max}(\rho)} = \frac{\sigma_{\lambda_{\max}(W)}}{\langle S \rangle} = 2^{4/3} n^{-5/3}$ for large n .

III. NUMERICAL RESULTS OF THE STATISTICS IN TWO SPIN MODELS

Model: We consider the following model for MBL, which is an XXZ spin- $\frac{1}{2}$ chain of L spins with a random z field and a small constant x field.

$$H = \frac{1}{2} \sum_{i=0}^{L-1} (\sigma_i^x \sigma_{i+1}^x + \sigma_i^y \sigma_{i+1}^y + \Delta \sigma_i^z \sigma_{i+1}^z) + \sum_i h_i \sigma_i^z + \Gamma \sum_i \sigma_i^x \quad (8)$$

h_i chosen to be *i.i.d.* uniformly random in $[-W, W]$. We consider both $\Gamma = 0$ and $\Gamma = 0.1$. For the $\Gamma = 0$ case, total S_z is conserved and we restrict ourselves to the half-filled sector with open boundary conditions. Since, we are interested in studying how *random* the model truly is in the ergodic phase, we need to break the S_z conservation without affecting the transition too much to see the effect of this conservation on the randomness.

We will refer to the model with $\Gamma = 0$ and $\Gamma = 0.1$ respectively as H_1 and H_2 . The model H_1 has been extensively studied and is believed to capture all essential properties of the MBL phase and the localization transition. For example, it is known that the model supports a MBL phase at strong disorder, an ergodic phase at weaker disorder, and an integrable point at zero disorder. For $\Delta = 1$ the transition was estimated to happen around $W \approx 3.5$ based on a variety of probes like the level statistics [7, 21, 49] and fluctuations of entanglement entropy [16]. Models with random fields along different directions have also been studied for example in [20, 50] and MBL transition with similar properties as H_1 was found.

Throughout the paper we have considered the middle one-third eigenstates for data. We have checked that there is no significant difference in the distributions we have computed if we instead choose a single eigenstate from the middle of the spectrum and many more disorder realizations. 500 disorder realizations are chosen for the $L = 14$, H_1 model and 100 disorder realizations for $L = 12$, H_2 model.

Let X be a discrete random variables with outcomes $1, 2, \dots, n$ and let $p_i = P(X = i)$. The Rényi entropy of order α , where $\alpha \geq 0$ and $\alpha \neq 1$ is defined as

$$H_\alpha(X) = \frac{1}{1-\alpha} \log \left(\sum_{i=1}^n p_i^\alpha \right).$$

In the limit of $\alpha \rightarrow \infty$ the Rényi entropy converges to the min-entropy,

$$H_\infty(X) = \min_i \{-\log p_i\} = -\log \max_i p_i. \quad (9)$$

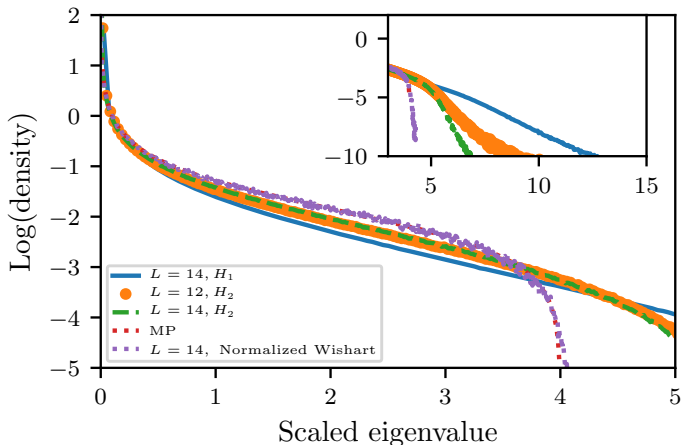


FIG. 1. Log of the scaled eigenvalue distribution for different L for H_2 and H_1 for $L = 14$, $W = 0.5$, MP refers to the Marchenko-Pastur distribution in Eqn. (7). The tail is shown in the inset.

The min-entropy, as its name indicates, is the smallest of the Rényi entropies and is the most conservative estimate of the information content of a random variable. In this paper we study the maximum of the entanglement spectrum, which essentially provides us with the min-entropy of entanglement.

A. Deviations from the Marchenko-Pastur distribution

We first compare the average density of the entanglement spectrum with the Marchenko-Pastur (MP) distribution. This is computed for $W = 0.5$ and shown for different L for H_2 and H_1 in Fig. (1). In the figures, scaled eigenvalue refers to the eigenvalues multiplied by the dimension $2^{L/2}$. For $L = 14$, in the H_2 model 20 disorder realizations have been used.

As is clear, breaking the total S_z conservation brings the distributions considerably closer to the MP distribution. While the density approaches the MP distribution for larger values of L , the tails show that the limiting distribution is perhaps close to MP, but different. Similar observations were reported in [22]. The Marchenko-Pastur has finite support from 0 to 4, but the distributions obtained from the data show exponential tails. Of course, the hard bound is obtained in the asymptotic $L \rightarrow \infty$ limit, however the softening of this for finite L [35] is too small in comparison to the tails observed here.

This is also reflected, as it should be, in the deviations of the moments from that of the MP distribution. The deviations from this are shown in Fig. (2) for H_2 , with the blue and orange curves representing respectively $M_k^{1/k}$ of the distribution obtained for $L = 12$, $W = 0.5$ and that of the Marchenko-Pastur distribution.

1. Deviation from gaussianity and normalized participation ratio

While looking for deviations shown by the entanglement spectrum statistics from the predictions of Wishart ensemble,

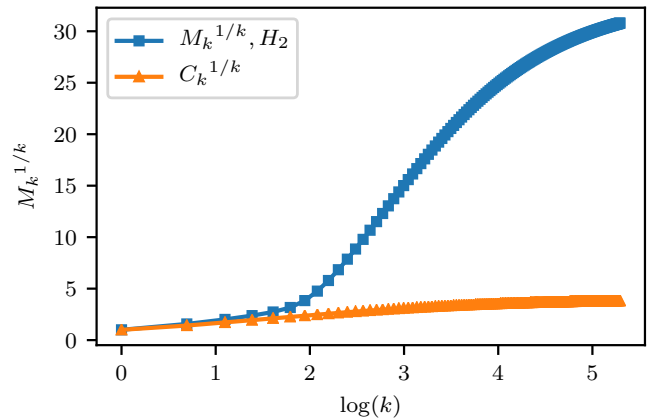


FIG. 2. Plot of $M_k^{1/k}$ with $\log(k)$ for $L = 12$, H_2 and $W = 0.5$ (squares). The other curve (triangles) depicts $C_k^{1/k}$ with $\log(k)$ and saturates to 4.

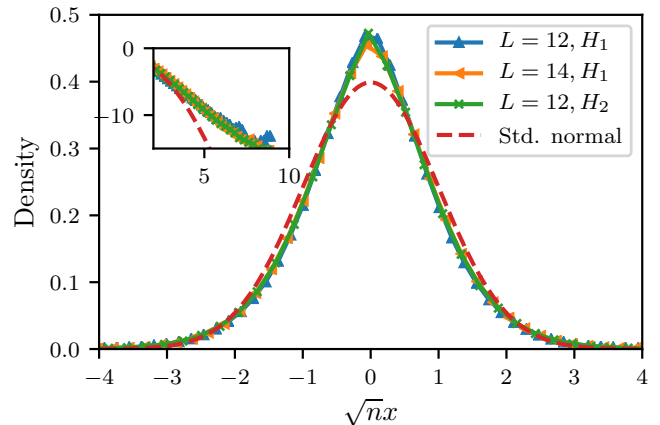


FIG. 3. Distribution of scaled eigenvector components \sqrt{nx} for $L = 14$, H_1 and $L = 12$, H_2 and disorder strength $W = 0.5$. The inset shows the tail, the y-axis of the inset represents the logarithm of the density.

it is natural to ask if the normalized components of eigenvectors (\sqrt{nx} , see Eqn. (3)) are themselves normally distributed, to begin with. While this would be the case if the GOE ensemble were to apply, although this is not a necessary condition for the MP distribution, due to its universality. As seen in Fig. (3), while the distributions approach Gaussian for increasing L , the fact that the logarithm of the distribution has near linear rather than quadratic tails, as seen in the inset, indicates that the limiting distribution is perhaps different. Interestingly, as seen in Fig. (4) the distribution of the normalized coefficients of the eigenvectors fits an exponential power distribution with p.d.f.

$$P(x) = \frac{\beta}{2\alpha\Gamma(1/\beta)} \exp\left(-\left|\frac{x}{\alpha}\right|^\beta\right) \quad (10)$$

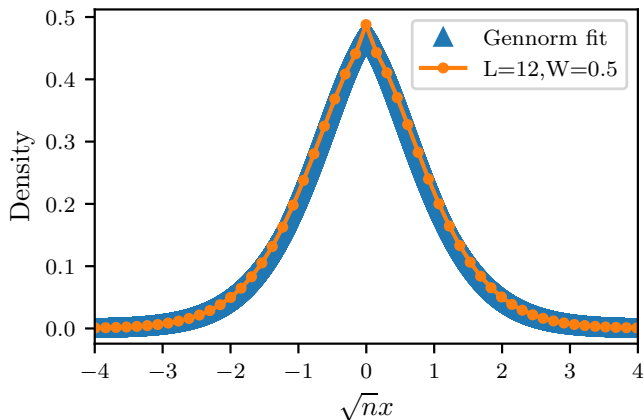


FIG. 4. Distribution of scaled eigenvector components \sqrt{nx} for $L = 12, H_2$ and $W = 0.5$, compared to a generalized normal distribution as in Eq. (10).

quite well. This is a generalization of the normal distribution ($\beta = 2$) with an additional shape parameter β . The β for the fits in the figure is to the leading order 1.5 and the scale factor $\alpha = 1.2$.

The deviation away from Gaussianity can be measured by the kurtosis of the distribution of scaled eigenvector coefficients. As the mean of the distribution is still close to zero, when computed for a single eigenvector, the kurtosis is equal to $\frac{1}{n} \sum_i (\sqrt{nx_i})^4$, which is just the normalized inverse participation ratio, $n \sum_i x_i^4$ with respect to the product basis in which H_1 and H_2 are diagonalized. Here we compute the inverse of this quantity, the normalized participation ratio (PR) which is the inverse of the kurtosis for different states. This mean value of the PR is known to be equal to $1/3$ for the GOE ensemble [51].

Also, random states are highly entangled, with the average entropy given by the Page value $\approx \ln n - \frac{1}{2}$ [27]. In Fig. (5) we show the entropy vs. PR plots for H_1 and H_2 for $L = 12$. The strong correlation between entropy and PR is clear. Thus most eigenstates are highly entangled with a participation ratio close to GOE. The mean PR for H_1 and H_2 are respectively, 0.259 and 0.264. The mean entropies are respectively 3.27 and 3.5, while the Page value ≈ 3.66 . Also as is clear from Fig. (5), in the model with total S_z conservation the PR and entropy have lower variance and are closer to random values as expected.

B. Deviations of the maximum from the Tracy-Widom distribution

Following the adaptations mentioned before, here we compare the maximum eigenvalue data after using a center and scaling respectively of $\frac{4}{n}$ and $2^{\frac{4}{3}} n^{-\frac{5}{3}}$ with $n = 2^{L/2}$. We have,

$$\lambda'_1 = \frac{(\lambda_1 - \frac{4}{n})}{2^{\frac{4}{3}} n^{-\frac{5}{3}}}. \quad (11)$$

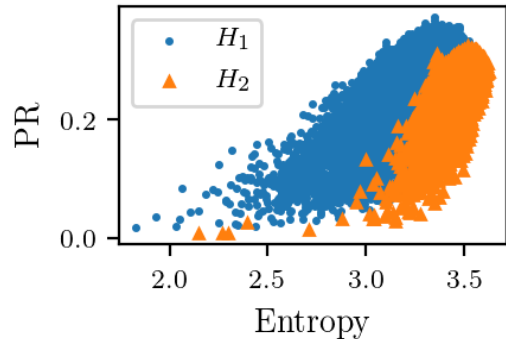


FIG. 5. Entanglement entropy vs participation ratio for $L = 12, H_1$, 500 realizations and $L = 12, H_2$, 100 realizations and $W = 0.5$.

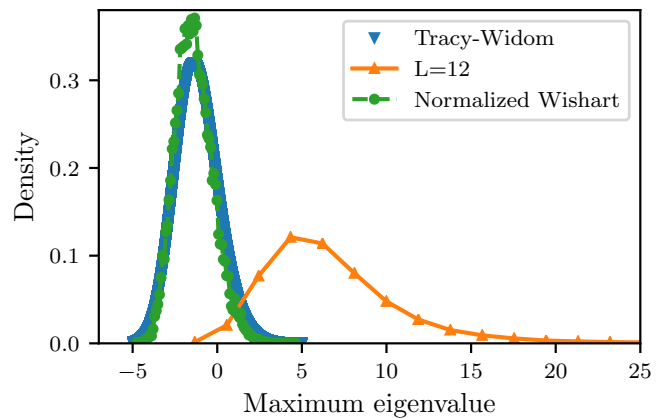


FIG. 6. Comparison of the distribution of the shifted-and-scaled maximum eigenvalue, λ'_1 , Eq. (11), with the Tracy-Widom distribution for $L = 12, H_2$ and $W = 0.5$. Shown for comparison is also the case of a (trace normalized) Wishart ensemble of dimension $2^{L/2} = 64$.

In order to compare for finite size effects, we also plot data from a trace normalized Wishart ensemble of the same dimensions. This is shown in Fig. (6). The Tracy-Widom distribution is obtained by using the R package called RMTstat [52].

As is clear, there are considerable deviations much beyond the finite size effects from the Tracy-Widom distribution, which implies that the correlations between eigenvalues of the reduced density matrix are not Wishart like. Thus, surprisingly even though the NNS distribution and number variance of the levels match GOE predictions for H_1 and H_2 ([7, 26]), a more rigorous test with respect to extreme statistics shows that the correlations between eigenvalues of the reduced density matrix of eigenvectors of the spin chains are much weaker. In Fig. (7) we show a fit of the data with the generalized extreme value distribution with the probability density function,

$$\begin{aligned} f(y; \xi) &= \exp(-(1 - \xi y)^{1/\xi}) (1 - \xi y)^{(1/\xi - 1)} \text{ for } \xi \neq 0 \\ &= \exp(-\exp(-y)) \exp(-y) \text{ for } \xi = 0. \end{aligned} \quad (12)$$

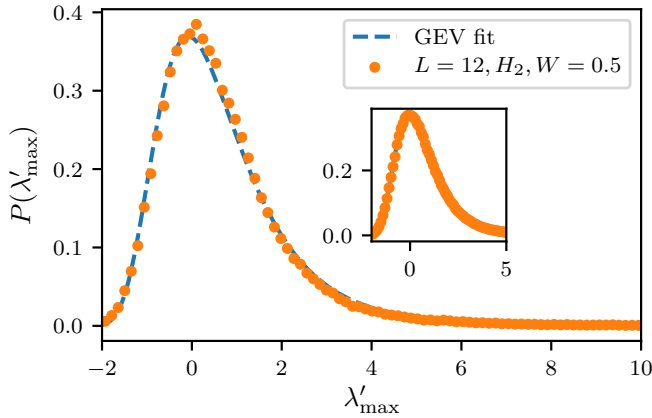


FIG. 7. Fit with the generalized extreme value distribution of the density of λ'_{\max} obtained from Hamiltonian H_2 ($L = 12$) and Hamiltonian H_1 ($L = 14$, inset), $W = 0.5$.

The shape parameter ξ takes a value of 0.069 and -0.086 respectively, for $L = 14$, H_1 data and $L = 12$, H_2 data for $W = 0.5$. The data has been centered and scaled by the location and scale parameters obtained by fitting a generalized extreme value distribution with free location and scale parameters (using Scipy) so that Eq. (12) can be used. In all the plots involving GEV we plot $\lambda'_{\max} = (\lambda_1 - \text{loc})/\text{scale}$ with the location (loc) and scale parameters for the fit produced in Table I. Note, that as the location and scale parameters for fitting the Tracy-Widom distribution, given by Eq. (11) are different from that of the GEV distribution, λ'_{\max} and λ'_1 are in general different. For the $L = 12, H_2$ data the location and scale parameters obtained from the fit are respectively 0.069, 0.007 while for the $L = 14, H_1$ data they are respectively 0.053, 0.008. This indicates that the best fitted distributions are close to Fisher-Tipett-Gumbel.

An interesting question is whether the deviation from the Wishart ensemble is due to the presence of low entropy and low PR states. To check for this we select eigenstates for the H_2 model, for $L = 12$ with entropy and PR respectively greater than 3.4 and 0.25. We then try to fit the maximum of the entanglement spectrum obtained from this data to the GEV distribution. The result is shown in Fig. (8), and the ξ value for the fit is 0.021 (location and scale parameters for the fit respectively being 0.073, 0.006), indicating that the distribution moves closer to being Fisher-Tipett-Gumbel, confirming that the correlations are not Wishart like even for the most random eigenstates. The distribution of the maximum obtained from this filtered data also show a deviation from the Tracy-Widom distribution similar to the deviation shown in Fig. (6), when we try to fit it using Eq. (11).

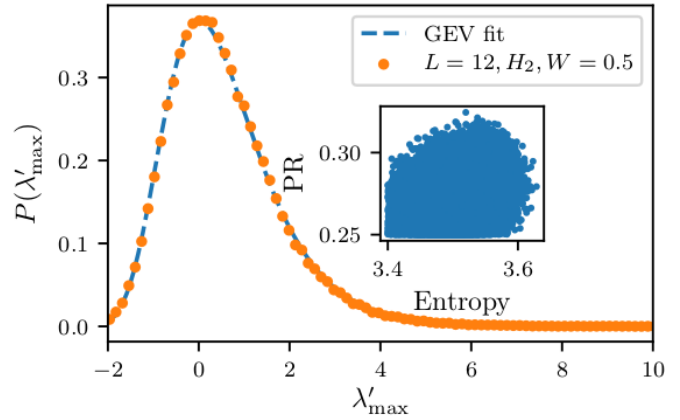


FIG. 8. Fit with the generalized extreme value distribution of the density of λ'_{\max} obtained from Hamiltonian H_2 for $W = 0.5$, $L = 12$, with an entropy and PR filter of respectively 3.4 and 0.25. Inset shows the entropy vs. PR scatter plot.

IV. EXTREME VALUE STATISTICS AWAY FROM THE ERGODIC PHASE

A. Persistence of GEV for moderate disorder strengths

Figure 9 inset shows the entropy-PR scatter plot for the H_2 model for disorder strength of $W = 1.0$. The entropy and PR distribution spreads considerably with the mean entropy and mean PR respectively lowering to become 3.37 and 0.17 respectively. The variance of entanglement entropy peaks as one approaches the transition, and thus the distributions are broadened. However, interestingly as shown in the main part of the same figure, the maximum still fits a GEV well, but with the ξ parameter being equal to -0.3021 .

As we move more towards the localized phase in W , the

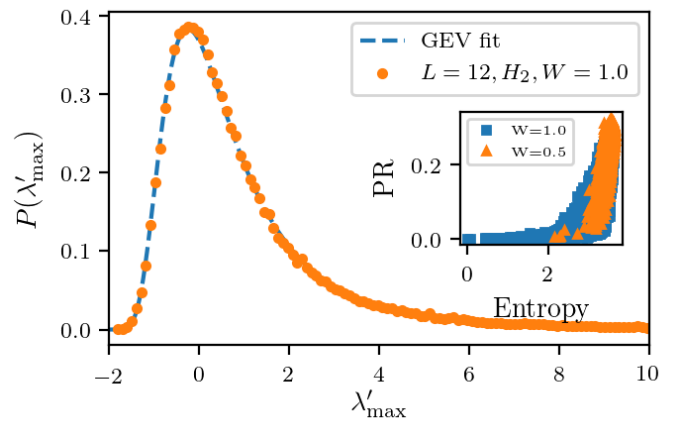


FIG. 9. Fit with the generalized extreme value distribution of the density of λ'_{\max} obtained from Hamiltonian H_2 for $W = 1.0$, $L = 12$. Inset shows Entropy vs PR for $L = 12$, the Hamiltonian H_2 , $W = 1.0$ (squares) and $W = 0.5$ (triangles)

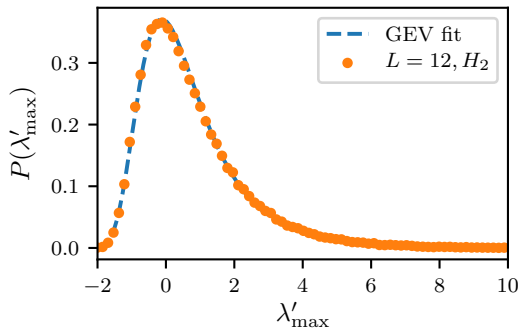


FIG. 10. Fit with the generalized extreme value distribution of the density of λ'_{\max} obtained from Hamiltonian H_2 for $W = 1.0$ for eigenstates with entropy greater than 3.0 and PR greater than 0.1.

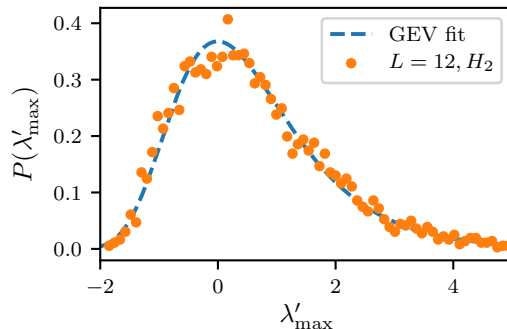


FIG. 12. Fit with the generalized extreme value distribution of the density of λ'_{\max} obtained from H_2 for $W = 2.0$, $L = 12$ for eigenstates with entropy greater than 3.0 and PR greater than 0.1.

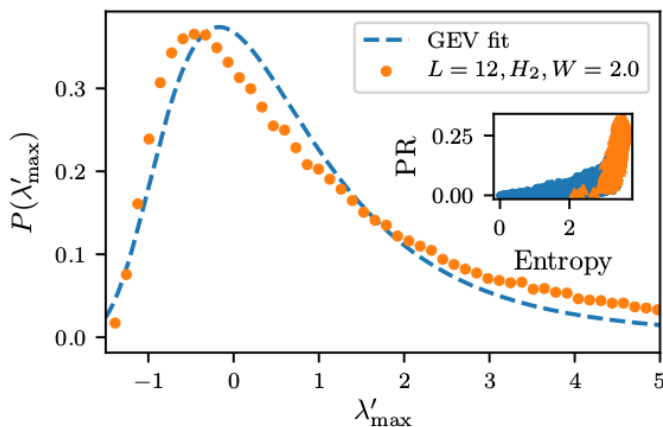


FIG. 11. Fit with the generalized extreme value distribution of the density of λ'_{\max} obtained from H_2 for $W = 2.0$, $L = 12$. Entropy vs PR scatter plot shown in inset for $L = 12$, the Hamiltonian H_2 , $W = 2.0$ (dots) and $W = 0.5$ (triangles).

eigenstates include many more low entropy and PR states indicating that they are almost localized and the maximum distribution seems to stop fitting a GEV. This is shown in Fig. (11) for $W = 2.0$. However, if we again weed out states with an entropy and PR respective lower than 3.0 and 0.1, the distribution again moves close to a GEV with $\xi = -0.004$, thus close to the Fisher-Tipett-Gumbel distribution, see Fig. 12.

The different values of the shape parameter ξ , and location and scale parameters used for centering and scaling the data before using Eq. (12) for the different fits for $L = 12$, H_2 model are collected in table I. Beyond about $W = 2.0$ and closer to the transition the GEV distribution itself deviate much more significantly.

TABLE I. ξ value for GEV fit

W	Filtered	ξ	loc	scale
0.5	No	-0.086	0.069	0.007
0.5	Yes	-0.021	0.073	0.006
1.0	No	-0.3021	0.092	0.018
1.0	Yes	-0.129	0.090	0.015
2.0	Yes	-0.004	0.103	0.021

B. Distribution of the maximum and second maximum of the entanglement spectrum and power laws in the MBL phase

For the sake of compactness and simplicity we present results only for the model H_2 without total spin or particle number conservation, although we have verified the same for the H_1 case as well. Figures (13) and (14) show the distribution of unscaled or shifted (“raw”) largest and second largest eigenvalue of the reduced density matrices, λ_1 and λ_2 , for $W = 1.5$ to 5 for the H_2 model. While for $W = 2.5$ the distribution of the largest eigenvalue λ_1 is rather broad, compared to the ergodic cases for $W = 3.0$ it displays a peak around $\lambda_1 = 1$, indicating the extreme nature of the extreme, as the other eigenvalues are then forced to be of far lesser significance. The dominance of the largest eigenvalue is indicative of entry into MBL regimes. A feature, we mention in passing, in the distribution of the maximum is the kink that develops at $\lambda_1 = 1/2$ around $W = 3.0$. Such a feature has also been seen in disorder averaged entanglement entropy as a resonance at $\ln 2$ in [53, 54], as well in weakly coupled chaotic systems [39], originating in fact from the behavior of the dominating largest eigenvalue.

As the disorder is increased the entanglement tends to the area-law and the largest eigenvalue tends to 1. As for the ergodic phase, with increasing disorder, the GEV statistics seems to apply well only if we filter states that are sufficiently ergodic, we expect that in the transition regime and in the MBL phase itself it will be harder to control this and as the largest eigenvalue has become $O(1)$ rather than of $O(1/n)$, we

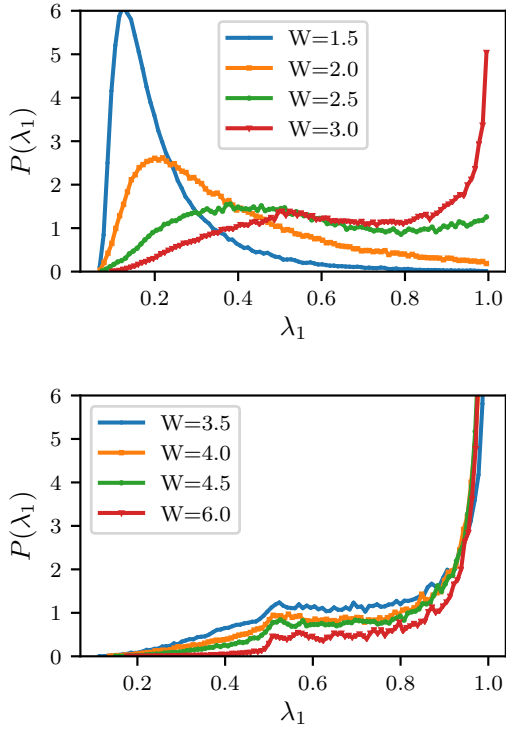


FIG. 13. Distribution of the largest eigenvalue λ_1 for the Hamiltonian H_2 , with $L = 12$ as the disorder strength is increased across the MBL transition.

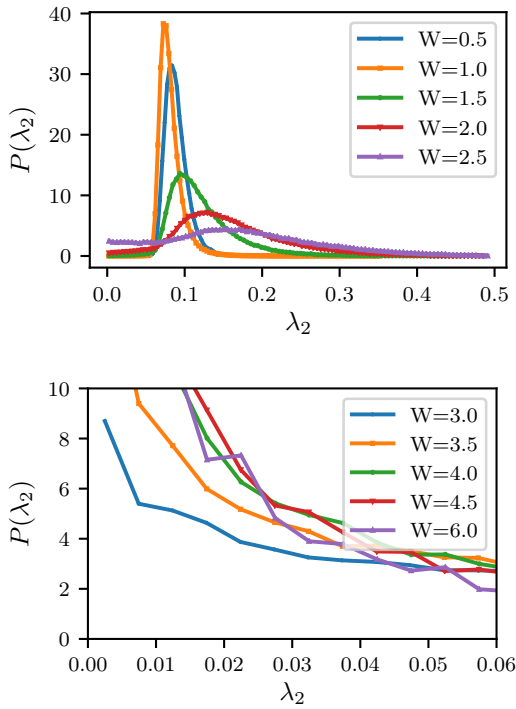


FIG. 14. Distribution of λ_2 for H_2 , $L = 12$.

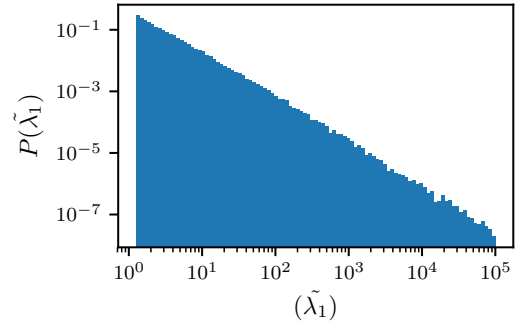


FIG. 15. Distribution of $\tilde{\lambda}_1$ for the Hamiltonian H_2 , and $L = 12$, with the disorder strength $W = 6$, the slope is ≈ -1.45

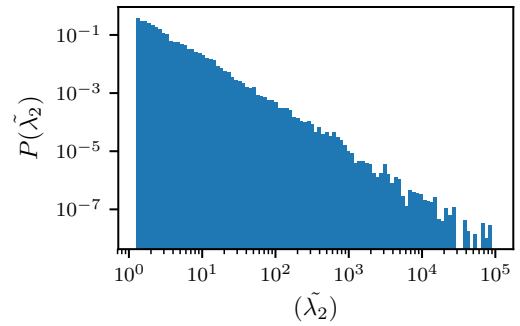


FIG. 16. Distribution of $\tilde{\lambda}_2$ for the Hamiltonian H_2 , and $L = 12$, with the disorder strength $W = 6$, the slope is ≈ -1.7 .

shift our analysis away from the GEV framework. For large disorder strengths W , we may take the view that the system is one consisting of spins with a Hamiltonian $\sum_i h'_i \sigma_i^z$ with h'_i being uniformly distributed in $[-1, 1]$ being subjected to weak interactions of the order $1/W$ due to the other terms. Thus the unperturbed Hamiltonian with $W = \infty$ has a Poisson spectrum on which there is weak coupling that leads to resonances between the bare states.

Recently a theory for such a scenario has been developed in [39] albeit in bipartite systems of weakly interacting chaotic systems. Notably, the noninteracting case there leads to a Poisson spectrum (despite the chaos), and the largest and second largest eigenvalues of the reduced density matrices of eigenstates were heavy tailed, including the Lévy distribution. In the present case of many-body MBL, the partition is bipartite as well, while the individual subsystems in the noninteracting case are not chaotic, but show Poisson statistics. The key elements of the analysis rely more on the Poisson nature of the uncoupled systems and hence it is interesting to compare the extreme value results from there. We will ignore an overall scaling by a “transition parameter” that is yet to be identified, if at all it exists, in the case of the MBL transition. Stable Lévy laws were seen, as a consequence of combining a regularized perturbation theory with the generalized central limit theorem [39] in the densities of somewhat transformed

quantities $\tilde{\lambda}_1 = g(\lambda_1)$ and $\tilde{\lambda}_2 = g(\lambda_2)$ where

$$g(x) = \frac{x(1-x)}{(1-2x)^2}. \quad (13)$$

Notice that $g(x) = g(1-x)$ and that for λ_1 , as it is typically close to 1 this is essentially $1 - \lambda_1$, and for λ_2 which is typically $\ll 1$, this is $\approx \lambda_2$ itself. However, we are really interested in the excursions of these values into non-typical values which happens frequently due to the power-laws. Note also that $\lambda_2 \leq 1/2$. Thus, applying the same transformation, Fig. (15) shows distribution for $\tilde{\lambda}_1$ for the H_2 model for $W = 6.0$, fairly deep in the MBL regime. An excellent power-law $\sim x^{-1.45}$ seems to be obtained, while Figure (16) shows the distribution of $\tilde{\lambda}_2$, for the H_2 model and once again a power law tail is evident and is close to $\sim x^{-1.7}$. These are close indeed to the ones derived in [39] which is $\sim x^{-3/2}$ corresponding to both the cases. Thus the extreme value statistics of MBL are also described by stable Lévy laws that manifest clearly on an appropriate transformation. There is no doubt that the comparisons with the perturbation results derived in [39] need to be more critical, but we are encouraged by the unmistakable similarities with the distribution of say λ_1 as it undergoes a transition into a localized regime, the broadening and the peak at $1/2$ are also seen in corresponding quantities of weakly coupled chaotic systems at appropriate coupling strengths which play the role of W .

V. CONCLUSIONS

In this work we have probed the randomness of the eigenstates of disordered spin chains showing the many-body localization transition, in the ergodic phase. We have used extreme statistics of the entanglement spectrum for this purpose. This is much more sensitive to the randomness of eigenstates compared to the distribution of the average density of the entanglement spectra which follows nearly a Marchenko-Pastur distribution for random states. For random states, the eigenvalues come from a trace constrained Wishart ensemble and the maximum follows the Tracy-Widom distribution after a suitable shift of center and scaling. We have found significant deviations from the Tracy-Widom law and the distribution we obtained instead fits the Fisher-Tippett-Gumbel distribution quite well. This is the distribution that maximal events of independent and identically distributed random variables follow after suitable rescaling. Our results thus indicate that even deep in the metallic phase the correlations in the entanglement spec-

tra are not as strong as those coming from truly random states and perhaps show signs of pre-localization. A natural question is if this is due to the presence of low entropy and participation ratio eigenstates present among the states which are closer to being random. But we have found that even the conditional distributions obtained after weeding out such states follow the generalized extreme value distribution and not the Tracy-Widom statistic. Even when the maximum distribution starts deviating significantly from GEV as we move towards the transition point, we found that the conditional distribution still follows GEV.

The fact that the Tracy-Widom law is not obtained even in the ergodic phase of a model with no conservation laws other than energy, maybe a generic feature of many-body systems. While quantities like the nearest neighbor spacing distributions or ratio of spacings may still be that of random matrices, the deviations will show in such properties of the eigenstates and the extreme value statistics could be the most stringent test of randomness, or at least one of them. It is possible though that further breaking conservation laws by Floquet kicked systems or even non-periodically driven systems may restore the extreme values to be of the Tracy-Widom type. Excellent agreement with the Marchenko-Pastur law and the Page value of subsystem entropy have been noted in these cases, for example see [55].

In the localized phase we shifted attention, motivated by recent results from a perturbation analysis of weakly coupled chaotic systems. Remarkably, we found that suitably transforming the largest and second largest eigenvalues lead to power-law distributions that match reasonably well with that derived earlier and indicate the applicability of Lévy stable laws in this context. This may also indicate the applicability of a regularized perturbation theory in the deep MBL regime, if not close to the transition. A work has appeared since the beginning of ours with identical motivations [56]. While our results unambiguously indicate the presence of the Fisher-Tippett-Gumbel law in the ergodic phase, the corresponding work shifts attention to the transition or localized regime. We have instead focused on an alternative strategy in the deep MBL phase wherein there are power-laws in the distribution of extreme eigenvalues (quite distinct from power laws in disorder averaged entanglement spectra itself plotted against the eigenvalue order as found in [21]). However, while we found it untenable with our data to fit GEV distributions for large values of W , the results of [56] indicate that this may still be possible. Apart from a closer comparison with such works, ours would hopefully contribute to an understanding of extreme value statistics in the spectra of many-body systems.

[1] P. W. Anderson, "Absence of diffusion in certain random lattices," *Phys. Rev.* **109**, 1492–1505 (1958).
 [2] D.M. Basko, I.L. Aleiner, and B.L. Altshuler, "Metal-insulator transition in a weakly interacting many-electron system with localized single-particle states," *Annals of Physics* **321**, 1126 – 1205 (2006).

[3] John Z. Imbrie, "Diagonalization and many-body localization for a disordered quantum spin chain," *Phys. Rev. Lett.* **117**, 027201 (2016).
 [4] Rahul Nandkishore and David A. Huse, "Many-body localization and thermalization in quantum statistical mechanics," *Annual Review of Condensed Matter Physics* **6**, 15–38 (2015),

- <https://doi.org/10.1146/annurev-conmatphys-031214-014726>.
- [5] David A. Huse, Rahul Nandkishore, and Vadim Oganesyan, “Phenomenology of fully many-body-localized systems,” *Phys. Rev. B* **90**, 174202 (2014).
 - [6] Jens H. Bardarson, Frank Pollmann, and Joel E. Moore, “Unbounded growth of entanglement in models of many-body localization,” *Phys. Rev. Lett.* **109**, 017202 (2012).
 - [7] Arijeet Pal and David A. Huse, “Many-body localization phase transition,” *Phys. Rev. B* **82**, 174411 (2010).
 - [8] Laumann C.R Yao N.Y and Vishwanath A., “Many-body localization protected quantum state transfer,” arXiv:1508.06995 (2015).
 - [9] M. Serbyn, M. Knap, S. Gopalakrishnan, Z. Papić, N. Y. Yao, C. R. Laumann, D. A. Abanin, M. D. Lukin, and E. A. Demler, “Interferometric probes of many-body localization,” *Phys. Rev. Lett.* **113**, 147204 (2014).
 - [10] Michael Schreiber, Sean S. Hodgman, Pranjal Bordia, Henrik P. Lüschen, Mark H. Fischer, Ronen Vosk, Ehud Altman, Ulrich Schneider, and Immanuel Bloch, “Observation of many-body localization of interacting fermions in a quasirandom optical lattice,” *Science* **349**, 842–845 (2015), <http://science.sciencemag.org/content/349/6250/842.full.pdf>.
 - [11] Luigi Amico, Rosario Fazio, Andreas Osterloh, and Vlatko Vedral, “Entanglement in many-body systems,” *Rev. Mod. Phys.* **80**, 517–576 (2008).
 - [12] J. Eisert, M. Cramer, and M. B. Plenio, “Colloquium: Area laws for the entanglement entropy,” *Rev. Mod. Phys.* **82**, 277–306 (2010).
 - [13] Alexei Kitaev and John Preskill, “Topological entanglement entropy,” *Phys. Rev. Lett.* **96**, 110404 (2006).
 - [14] Xiao-Gang Wen, “Quantum orders in an exact soluble model,” *Phys. Rev. Lett.* **90**, 016803 (2003).
 - [15] Jens H. Bardarson, Frank Pollmann, and Joel E. Moore, “Unbounded growth of entanglement in models of many-body localization,” *Phys. Rev. Lett.* **109**, 017202 (2012).
 - [16] Jonas A. Kjäll, Jens H. Bardarson, and Frank Pollmann, “Many-body localization in a disordered quantum ising chain,” *Phys. Rev. Lett.* **113**, 107204 (2014).
 - [17] Soumya Bera and Arul Lakshminarayan, “Local entanglement structure across a many-body localization transition,” *Phys. Rev. B* **93**, 134204 (2016).
 - [18] Hui Li and F. D. M. Haldane, “Entanglement spectrum as a generalization of entanglement entropy: Identification of topological order in non-abelian fractional quantum hall effect states,” *Phys. Rev. Lett.* **101**, 010504 (2008).
 - [19] Zhi-Cheng Yang, Claudio Chamon, Alioscia Hamma, and Eduardo R. Mucciolo, “Two-component structure in the entanglement spectrum of highly excited states,” *Phys. Rev. Lett.* **115**, 267206 (2015).
 - [20] Scott D. Geraedts, Rahul Nandkishore, and Nicolas Regnault, “Many-body localization and thermalization: Insights from the entanglement spectrum,” *Phys. Rev. B* **93**, 174202 (2016).
 - [21] Maksym Serbyn, Alexios A. Michailidis, Dmitry A. Abanin, and Z. Papić, “Power-law entanglement spectrum in many-body localized phases,” *Phys. Rev. Lett.* **117**, 160601 (2016).
 - [22] Francesca Pietracaprina, Giorgio Parisi, Angelo Mariano, Savio Pascasio, and Antonello Scardicchio, “Entanglement critical length at the many-body localization transition,” *Journal of Statistical Mechanics: Theory and Experiment* **2017**, 113102 (2017).
 - [23] Y. Y. Atas, E. Bogomolny, O. Giraud, and G. Roux, “Distribution of the ratio of consecutive level spacings in random matrix ensembles,” *Phys. Rev. Lett.* **110**, 084101 (2013).
 - [24] Madan Lal Mehta, *Random Matrices*, 3rd ed. (2004).
 - [25] Marie-Joya Giannoni, Andre Voros, and Jean Zinn-Justin, *Chaos and quantum physics, Volume 52 of Les Houches Summer School Proceedings Series* (North-Holland, 1991).
 - [26] Corentin L. Bertrand and Antonio M. García-García, “Anomalous thouless energy and critical statistics on the metallic side of the many-body localization transition,” *Phys. Rev. B* **94**, 144201 (2016).
 - [27] Don N. Page, “Average entropy of a subsystem,” *Phys. Rev. Lett.* **71**, 1291–1294 (1993).
 - [28] Craig A. Tracy and Harold Widom, “On orthogonal and symplectic matrix ensembles,” *Communications in Mathematical Physics* **177**, 727–754 (1996).
 - [29] R. A. Fisher and L. H. C. Tippett, “Limiting forms of the frequency distribution of the largest or smallest member of a sample,” *Mathematical Proceedings of the Cambridge Philosophical Society* **24**, 180 (1928).
 - [30] E J Gumbel, *Statistics of extremes* (Dover Publications Inc., New York, 2004).
 - [31] M. R. Leadbetter and Holger Rootzen, “Extremal theory for stochastic processes,” *The Annals of Probability* **16**, 431–478 (1988).
 - [32] A. De Luca and A. Scardicchio, “Ergodicity breaking in a model showing many-body localization,” *EPL (Europhysics Letters)* **101**, 37003 (2013).
 - [33] Satya N. Majumdar, Oriol Bohigas, and Arul Lakshminarayan, “Exact minimum eigenvalue distribution of an entangled random pure state,” *Journal of Statistical Physics* **131**, 33–49 (2008).
 - [34] Satya N. Majumdar, *Extreme eigenvalues of Wishart matrices: application to entangled bipartite system*, Oxford Handbook of Random Matrix Theory (Oxford University Press, 2011).
 - [35] Hiroto Kubotani, Satoshi Adachi, and Mikito Toda, “Exact formula of the distribution of schmidt eigenvalues for dynamical formation of entanglement in quantum chaos,” *Phys. Rev. Lett.* **100**, 240501 (2008).
 - [36] Pierpaolo Vivo, “Largest schmidt eigenvalue of random pure states and conductance distribution in chaotic cavities,” *Journal of Statistical Mechanics: Theory and Experiment* **2011**, P01022 (2011).
 - [37] Santosh Kumar, Bharath Sambasivam, and Shashank Anand, “Smallest eigenvalue density for regular or fixed-trace complex wishart-laguerre ensemble and entanglement in coupled kicked tops,” *Journal of Physics A: Mathematical and Theoretical* **50**, 345201 (2017).
 - [38] Peter J Forrester and Santosh Kumar, “Recursion scheme for the largest β -wishart-laguerre eigenvalue and landauer conductance in quantum transport,” *Journal of Physics A: Mathematical and Theoretical* **52**, 42LT02 (2019).
 - [39] Steven Tomsovic, Arul Lakshminarayan, Shashi C. L. Srivastava, and Arnd Bäcker, “Eigenstate entanglement between quantum chaotic subsystems: Universal transitions and power laws in the entanglement spectrum,” *Phys. Rev. E* **98**, 032209 (2018).
 - [40] Arul Lakshminarayan, Steven Tomsovic, Oriol Bohigas, and Satya N. Majumdar, “Extreme statistics of complex random and quantum chaotic states,” *Phys. Rev. Lett.* **100**, 044103 (2008).
 - [41] Iain M. Johnstone, “On the distribution of the largest eigenvalue in principal components analysis,” *The Annals of Statistics* **29**, 295–327 (2001).
 - [42] Michael A. Nielsen and Isaac L. Chuang, *Quantum Computation and Quantum Information: 10th Anniversary Edition*, 10th ed. (Cambridge University Press, New York, NY, USA, 2011).
 - [43] Karol Zyczkowski and Hans-Jürgen Sommers, “Induced measures in the space of mixed quantum states,” *Journal of Physics*

- A: Mathematical and General **34**, 7111–7125 (2001).
- [44] I. Bengtsson and K. Życzkowski, *Geometry of Quantum States: An Introduction to Quantum Entanglement* (Cambridge University Press, 2017).
- [45] Jean Ginibre, “Statistical ensembles of complex, quaternion, and real matrices,” *J. Mathematical Phys.* **6**, 440–449 (1965).
- [46] Terence Tao and Van Vu, “Random covariance matrices: Universality of local statistics of eigenvalues,” *Ann. Probab.* **40**, 1285–1315 (2012).
- [47] F. Haake, *Quantum Signatures of Chaos*, Physics and astronomy online library (Springer, 2001).
- [48] Ion Nechita, “Asymptotics of random density matrices,” *Annales Henri Poincaré* **8**, 1521–1538 (2007).
- [49] David J. Luitz, Nicolas Laflorencie, and Fabien Alet, “Many-body localization edge in the random-field heisenberg chain,” *Phys. Rev. B* **91**, 081103 (2015).
- [50] Nicolas Regnault and Rahul Nandkishore, “Floquet thermalization: Symmetries and random matrix ensembles,” *Phys. Rev. B* **93**, 104203 (2016).
- [51] T. A. Brody, J. Flores, J. B. French, P. A. Mello, A. Pandey, and S. S. M. Wong, “Random-matrix physics: spectrum and strength fluctuations,” *Rev. Mod. Phys.* **53**, 385–479 (1981).
- [52] Iain M. Johnstone, Zongming Ma, Patrick O. Perry, and Morteza Shahram, *RMTstat: Distributions, Statistics and Tests derived from Random Matrix Theory* (2014), r package version 0.3.
- [53] David J. Luitz, “Long tail distributions near the many-body localization transition,” *Phys. Rev. B* **93**, 134201 (2016).
- [54] S. P. Lim and D. N. Sheng, “Many-body localization and transition by density matrix renormalization group and exact diagonalization studies,” *Phys. Rev. B* **94**, 045111 (2016).
- [55] Sunil K. Mishra and Arul Lakshminarayan, “Resonance and generation of random states in a quenched ising model,” *EPL (Europhysics Letters)* **105**, 10002 (2014).
- [56] Wouter Buijsman, Vladimir Gritsev, and Vadim Cheianov, “Gumbel statistics for entanglement spectra of many-body localized eigenstates,” *Phys. Rev. B* **100**, 205110 (2019).